Environmental Research 207 (2022) 112165

Contents lists available at ScienceDirect

Environmental Research

journal homepage: www.elsevier.com/locate/envres

Phytoplankton growth rates in the Amundsen Sea (Antarctica) during summer: The role of light

Youngju Lee, Jinyoung Jung, Tae Wan Kim, Eun Jin Yang *, Jisoo Park

Division of Ocean Sciences, Korea Polar Research Institute, 26 Songdomirae-ro, Yeonsu-gu, Incheon, 21990, Republic of Korea

ARTICLE INFO

Keywords:
Phytoplankton
Growth rate
Phaeocystis antarctica
Diatoms
Amundsen Sea
Light limitation

ABSTRACT

In the Amundsen Sea, significant global warming accelerates ice melt, and is consequently altering many ocean properties such as sea ice concentration, surface freshening, water column stratification, and underwater light properties. To examine the influence of light, which is one of the fundamental factors for phytoplankton growth, incubation experiments and field surveys were performed during the austral summer of 2016. In the incubation experiments, phytoplankton abundance and carbon biomass significantly increased with increasing light levels, probably indicating light limitation. Growth rates of the small pennates (mean 0.42 d^{-1}) increased most rapidly with an increase in light, followed by those of *Phaeocystis antarctica* (0.31 d^{-1}), and the large diatoms (0.16 d^{-1}). A short-term study during the field survey showed that phytoplankton distribution in the surface layer was likely controlled by different responses to light and the sinking rate of each species. These results suggest that the approach adopted by previous studies of explaining phytoplankton ecology as a characteristic of two major taxa, namely diatoms and *P. antarctica*, in the coastal Antarctic waters might cause errors owing to oversimplification and misunderstanding, since diatoms comprise several species that have different ecophysiological characteristics.

1. Introduction

The Amundsen Sea is the current hotspot of rapidly thinning ice shelves in the West Antarctica owing to global warming (Rignot et al., 2013). Basal melt water from the ice shelves supplies iron to the coastal waters and enhances the surface freshening in this area (Gerringa et al., 2012; Silvano et al., 2018). Warming associated with sea ice melting could have a significant impact on light transmission between the air and sea surface (Samuel et al., 2017), and fine suspended particles from ice melting could have an impact on the underwater light field (Pan et al., 2019). The Amundsen Sea Low has deepened in recent decades, influencing the West Antarctic climate via atmospheric teleconnections (Dotto et al., 2020), often leading to anomalies of opposite signs in temperature, sea ice, and precipitation in the West Antarctic coast (Holland et al., 2018; Raphael et al., 2016). Changes in precipitation and sea ice distribution due to the deepening of the Amundsen Sea Low could cause changes in cloud and sea ice concentrations, which could have an effect on the insolation and light penetration to the sea surface, respectively. Consequently, biological changes are expected to occur because these physical, chemical, and climatological changes, especially light and dissolved iron availability, have a direct effect on phytoplankton growth and community distribution in this area (Alderkamp et al., 2012b; Lee et al., 2016).

The Amundsen Sea Polynya (ASP)[1] is the most productive of the Antarctic coastal polynya systems, which are areas of open waters surrounded by ice (Arrigo and van Dijken, 2003). It is well known that the phytoplankton community is dominated by the prymnesiophyte *Phaeocystis antarctica* and diatoms, with their spatial and temporal distributions occurring differently (Fragoso and Smith Jr, 2012; Lee et al., 2016). They have different carbon (C)[2] uptake rates, macronutrient demands, and iron availability as well as different food preferences for krill; thus, compositional changes have a significant impact on biogeochemical cycles and pelagic food web structures (Arrigo et al., 1999; Yang et al., 2019; Zhu et al., 2016). There have been many studies on environmental factors controlling the phytoplankton community distribution in the coastal waters of the rapidly changing ASP. In recent years, these studies have been mainly focused on sea ice concentration, mixed layer depth, and iron (Alderkamp et al., 2015; Arrigo et al., 2014;

* Corresponding author.
E-mail address: ejyang@kopri.re.kr (E.J. Yang).

[1] ASP: Amundsen Sea Polynya.

[2] C: Carbon.

https://doi.org/10.1016/j.envres.2021.112165
Received 16 February 2021; Received in revised form 26 August 2021; Accepted 29 September 2021
Available online 4 October 2021

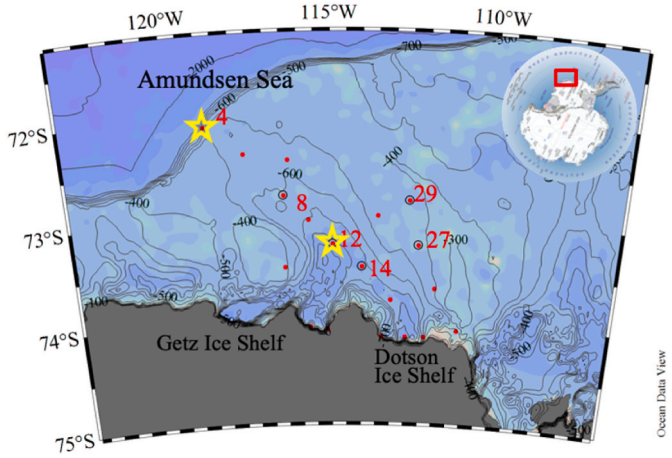

Fig. 1. Sampling stations and bathymetry in the Amundsen Sea, Antarctica. Black circles indicate the sampling stations and yellow stars indicate the stations for incubation experiments from January to February 2016. (For interpretation of the references to color in this figure legend, the reader is referred to the Web version of this article.)

that control the summer phytoplankton bloom and to examine how the phytoplankton community in the ASP responds under various light conditions. In order to investigate short-term changes in environmental and phytoplankton properties, five stations were visited twice in January and February 2016, a season in which environmental factors such as sea surface temperature, nutrient concentration, and insolation are rapidly changing after the phytoplankton bloom in this area (Arrigo et al., 2012; Oliver et al., 2019). The incubation experiments were conducted using seawater in the ASP during the cruise, and the growth rates of the phytoplankton species, pigment contents, and nutrient concentrations were determined in the experimental bottles. This research provides insights into how perpetual changes in light might alter the phytoplankton biomass and composition in the currently changing ASP. In addition, we could use this information to better parameterize models and to predict future biogeochemical cycles and food web structures in this area.

2. Materials and methods

2.1. Incubation experiments and field survey

Experiments and field surveys were conducted from 15 January to February 7, 2016 during the Amundsen cruise onboard the icebreaker research vessel Araon (Fig. 1). Phytoplankton response to variable light intensities were investigated through incubation experiments. Spatial differences in the composition of phytoplankton species have been previously reported in this area (Lee et al., 2016), thus two sampling stations on the shelf break and the ASP were chosen for the experiments as representative areas. For the experiments, 100 L of seawater was collected from the Amundsen Sea coastal area, one in the shelf break (Station 4) and one in the ASP (Station 12), using the Niskin bottles attached to the CTD at 20 and 10 m, respectively, to represent the euphotic depth. The euphotic depths at which the photosynthetically active radiation (PAR)[3] was 1 % of its surface value were 20.5 m (Station 4) and 14.5 m (Station 12). Water samples were gently filtered through a 200-μm mesh screen to minimize the grazing pressure of the large zooplankton and were collected in 10-L acid-washed transparent polycarbonate bottles (Nalgene, USA) under dim light to prevent light shock. Polycarbonate bottles allowed PAR radiation to pass through, but filtered out UVB and UVA radiation, indicating that they had minimizing

Table 1
Macronutrients (μM) and photosynthetic pigment concentrations (μgL^{-1}) under the different light treatments.

Experiments	Experiment 1				Experiment 2			
Time	Initial	Day 8			Initial	Day 9		
Light conditions		1 %	30 %	50 %		1 %	30 %	50 %
NH_4 (μM)	1.23	0.31 ± 0.28	4.00 ± 1.15	1.55 ± 0.82	0.85	2.51 ± 0.34	5.19 ± 0.38	3.34 ± 0.26
NOx (μM)	21.80	21.17 ± 0.26	3.21 ± 4.18	BDL	21.90	19.37 ± 0.28	0.83 ± 1.02	BDL
P (μM)	1.67	1.60 ± 0.03	0.55 ± 0.11	0.28 ± 0.05	1.66	1.69 ± 0.01	0.51 ± 0.12	0.28 ± 0.04
Si (μM)	77.81	77.00 ± 0.35	56.57 ± 0.17	58.16 ± 2.13	82.04	80.77 ± 0.38	50.63 ± 3.93	43.04 ± 0.61
NOx:P*	13.05	13.34 ± 0.31	8.82 + 3.29	3.91 ± 1.85	13.22	11.88 ± 0.29	6.93 ± 3.34	4.55 ± 0.62
dNOx (μM)*		1.17 ± 0.11	14.83 ± 3.86	18.81 ± 1.60		1.05 ± 0.11	14.95 ± 4.73	18.01 ± 0.49
dP (μM)*		0.12 ± 0.04	0.91 ± 0.13	0.93 ± 0.07		−0.10 ± 0.71	0.71 ± 0.23	0.80 ± 0.01
dSi (μM)*		−0.15 ± 0.50	13.82 ± 1.21	14.89 ± 2.05		1.85 ± 0.57	16.70 ± 6.66	22.10 ± 0.31
Chl-a (μgL^{-1})	1.93	1.87 ± 0.22	4.84 ± 1.22	4.37 ± 0.45	3.03	4.12 ± 0.10	6.66 ± 0.52	9.31 ± 2.37
Fuco/Chl-a	1.00	1.29 ± 0.11	1.55 ± 0.39	1.43 ± 0.18	2.13	1.55 ± 0.01	2.21 ± 0.14	2.12 ± 0.15
Hex-fuco/Chl-a	0.62	0.58 ± 0.01	1.14 ± 0.39	1.36 ± 0.20	0.15	0.09 ± 0.02	0.23 ± 0.01	0.15 ± 0.03
DD + DT/Chl-a	0.10	0.08 ± 0.00	0.25 ± 0.04	0.34 ± 0.01	0.24	0.10 ± 0.00	0.27 ± 0.00	0.20 ± 0.04

Note. Average and standard deviation (±SD) of macronutrients (μM) and photosynthetic pigment concentrations (μgL^{-1}) in the initial and the final days of the incubations under the different light treatments. DIN, dissolved inorganic nitrogen (ammonia + nitrite + nitrate); NH_4, ammonium; NOx, nitrite + nitrate; P, phosphate; Si, silicate; NOx:P, nitrite + nitrate:P; Fuco, fucoxanthin; Hex-fuco, 19′-hexanoyloyfucoxanthin; DD + DT, diadinoxanthin + diatoxanthin; BDL, below the detection limit. The "d" before the nutrients and the superscript * indicate the drawdown (d) of nutrient concentrations on day 6 (*) from the initials.

Oliver et al., 2019), but the effect of light has rarely been explored, despite being the major controller of phytoplankton growth (Park et al., 2017).

As Antarctica is difficult to access, autecological studies have also been extensively conducted in many laboratories to reveal the ecological characteristics of the two dominant groups using *Fragilariopsis cylindrus* and *P. antarctica* as the type species of diatoms and prymnesiophytes, respectively (Alderkamp et al., 2012a; Kropuenske et al., 2009; Mills et al., 2010). *P. antarctica* is a predominant species in prymnesiophytes, while diatoms comprise several species, and each of these species has been reported to have various photophysiological properties in western Antarctica. In general, significant inter- and intra-specific variations in diatoms exist in response to many factors such as geographical location, temperature, iron concentration, including light intensity (Rynearson and Armbrust, 2004; Strzepek and Harrison, 2004; Whittaker et al., 2012). *F. cylindrus* is one of the major diatoms in the West Antarctic coastal waters (Kang and Fryxell, 1992), but it illustrates the dangers of using a sole strain of a cultured phytoplankton species to represent an entire diatom group in the Antarctic ecosystem, especially when compared with *P. antarctica*.

The aim of the present study was to explore environmental factors

[3] PAR: Photosynthetically active radiation.

UV effects on phytoplankton growth. All procedures for the preparation and incubation were completed within 30 min after the CTD cast. Three incubators were screened to 99 %, 70 %, and 50 % of incident light, respectively, using sunscreen filters (LEE filters, Andover, UK) and were kept at the sea surface temperature by continuous flushing from the ship's underway seawater supply system. Triplicate bottles for experiment 1 (exp. 1)[4] and duplicate bottles for experiment 2 (exp. 2)[5] were incubated in the deck incubators under different light levels (1 %, 30 %, and 50 % PAR of its incident irradiance) for 8–9 days. Nothing was added to the bottles because of the very high initial concentrations of macronutrients present in the collected seawater (Table 1). Samples for the nutrients were taken once in 2 d, and samples for chlorophyll-a (chl-a)[6] were taken at time zero, on day 6, and on the final days of the incubations. Samples for microscopy and photosynthetic pigments were taken on the initial and final days of the experiments. At the beginning of the incubation period, 10 L of seawater was dispensed to each 10-L bottle, and approximately 8 L of seawater remained in the bottles just before the final sampling took place.

To investigate short-term changes in the environmental and phytoplankton data, five stations were visited twice at the beginning (mid-January) and the end (early February) of the cruise. Measurements from casts of a Seabird 911 plus model CTD (Sea-Bird Scientific, USA) include water column properties such as temperature, salinity, and chlorophyll fluorescence. The discrete water samples for the estimation of the nutrient and chl-a concentrations, phytoplankton species composition, cell abundance, and C biomass were collected from five or six layers in the upper 100 m.

2.2. Sample processing

The macronutrient concentrations including nitrate + nitrite (NOx),[7] ammonium, phosphate (P),[8] and silicate (Si)[9] were measured onboard using standard colorimetric methods adapted for use with a four-channel auto-analyzer (QuAAtro; Seal Analytical, USA) according to the manufacturer's instructions (QuAAtro Applications). Chl-a was determined onboard using samples immediately filtered through glass-fiber filter paper (47 mm; Gelman GF/F), extracted with 90 % acetone for 24 h (Parsons et al., 1984), and then measured in a fluorometer (Trilogy, Turner Designs, USA), previously calibrated against pure chl-a (Sigma). Samples for pigments were filtered through a 47-mm GF/F Whatman filter and stored in a freezer at −80 °C. The filters were extracted with 3 mL of 100 % acetone, ultrasonicated for 30 s, and maintained at 4 °C in the dark for 15 h. Debris was removed by filtering through a 0.45-μm Teflon syringe filter. Immediately before injection, the extracts were diluted with distilled water (1 mL of extract + 0.3 mL of water) to avoid peak distortion of the first eluting pigments. Pigments were assessed with high-performance liquid chromatography (HPLC)[10] following the method of Zapata et al. (2000). Before the analysis, the instrument (series 1200 chromatographic system; Agilent, Germany) was calibrated using the following standard pigments (DHI, Denmark): chl-a, chl-b, chl-c2, chl-c3, 19-butanoyloxyfucoxanthin, fucoxanthin (fuco),[11] 19-hexanoyloxyfucoxanthin (hex-fuco),[12] diadinoxanthin (DD),[13] dinoxanthin, diatoxanthin (DT),[14] neoxanthin, prasinoxanthin, violaxanthin, alloxanthin, zeaxanthin, lutein, and peridinin. A 250 mm × 4.6 mm, 5 μm, C8 column (XDB-C8; Agilent, USA) was used for the pigment separation. Pigments were identified by their retention times and absorbance spectra. The retention times were compared with those of pure standards and those reported in Zapata et al. (2000). After determining the pigment concentrations, the response factor was calculated as the weight of the standard injected divided by the area of the pigment. The concentrations of standard pigments were calibrated by spectrophotometry with the known absorption coefficients from Jeffrey et al. (1997). Surface PAR was determined using a quantum sensor (LI-1400, LI-COR Inc., USA) every 5 min during the cruise. Mixed layer depth (MLD)[15] was determined from the maximum of the Brunt-Väisälä buoyancy frequency (Carvalho et al., 2017).

To enumerate the phytoplankton taxonomic composition, cell abundance, C biomass, and taxon specific growth rate, water samples were subsampled using 200-mL high-density polyethylene bottles, preserved with glutaraldehyde (final concentration 1 %), and stored at 4 °C until processed as follows: Sample volumes of 20–100 mL were filtered through Nuclepore filters (0.8-μm pore size, black, 25-mm diameter) until 5 mL were remaining in the filtration tower. Concentrated DAPI (50 μg mL^{-1} final concentration) was then added to this remaining volume, which was also filtered after a brief (5-s) incubation (Taylor et al., 2011). The filters were mounted on glass slides with immersion oil and cover slips. Microphytoplankton (>20 μm), nanophytoplankton (5–20 μm), and picophytoplankton (2–5 μm) and dinoflagellates were enumerated using epifluorescence microscopy with blue light excitation (Olympus, BX 51). Phytoplankton was distinguished from heterotrophs by the presence of chlorophyll, which was visualized as red fluorescence under blue light illumination. The cells were counted in random fields at magnifications of 200–1600 × until a total of 50 fields or 300 cells were observed. Phytoplankton cell dimensions were measured to the nearest 1 μm during the microscopy observations. The values were used for subsequent estimations of biovolume according to the geometric shapes of the cells. C biomass was estimated from the cell biovolume using modified Eppley equations for diatoms and other phytoplankton (Hillebrand et al., 1999; Smayda, 1978). The conversion factor was used to transform the cell numbers of solitary *P. antarctica* into C biomass (3.33 $pgCcell^{-1}$) (Mathot et al., 2000). Because colonies can break during processing, we were not able to determine whether individual *P. antarctica* cells were previously colonial or always single cells. Most *P. antarctica* was present as solitary flagellated cells ranging in size from 1 to 6 μm. The taxon-specific growth rate (expressed as d^{-1}) was calculated as $\mu = (\ln N_t - \ln N_0)/t$, where N_0 and N_t are the cell numbers of phytoplankton species at the beginning and end of the incubation periods, respectively, and t is the duration of the incubation periods.

2.3. Statistical analysis

The statistical analyses were carried out using R4.0.5 software (R Development Core Team, http://www.r-project.org) and supplemented with the *vegan* package. The taxon-specific gross growth rate of the major phytoplankton species was compared at three light levels by performing an analysis of variance test (ANOVA test, *kruskal* function in R), because most of the data were not normally distributed. A Bray-Curtis dissimilarity matrix was constructed from the log-transformed phytoplankton species abundance and non-metric multidimensional scaling (NMDS) was performed using the *metaMDS* function, which was visualized using the *ggplot2* package. Differences between the phytoplankton composition of the samples were determined using an analysis of similarities test (ANOSIM test, *anosim* function), from the log-transformed phytoplankton species abundance. To analyze the correlation between phytoplankton species abundance and environmental variables that included water temperature, salinity, nutrient

[4] Exp. 1: Experiment 1.
[5] Exp. 2: Experiment 2.
[6] Chl-a: Chlorophyll-a.
[7] NOx: Nitrate + Nitrite.
[8] P: Phosphate.
[9] Si: Silicates.
[10] HPLC: High-performance liquid chromatography.
[11] fuco: Fucoxanthin.
[12] hex-fuco: 19-hexanoyloxyfucoxanthin.
[13] DD: Diadinoxanthin.
[14] DT: Diatoxanthin.
[15] MLD: Mixed layer depth.

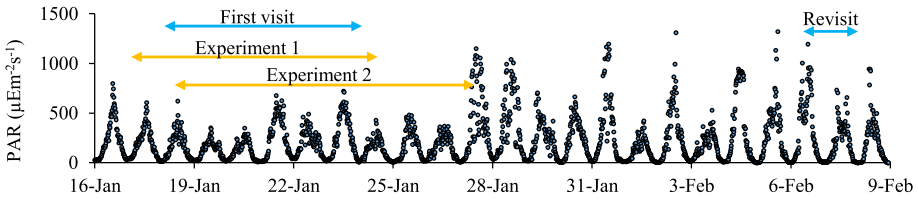

Fig. 2. Photosynthetically active radiation, PAR ($\mu Em^{-2}s^{-1}$) throughout the experiments and field survey. Yellow arrows indicate the incubation periods for each experiment. Blue arrows indicate the sampling periods for the first visit and the revisit at five stations in the Amundsen Sea polynya. (For interpretation of the references to color in this figure legend, the reader is referred to the Web version of this article.)

concentration, and light conditions, the *envfit* function was used to fit the variables into the NMDS ordination from log-transformed abiotic data. In order to determine the indicator species of the phytoplankton community between visits, indicator species analysis was applied using the *indicspecies* package.

3. Results and discussion

3.1. Initial conditions

Bioassay experiments were conducted in two distinct oceanographic regions: (i) exp. 1: relatively colder (−1.55 °C and 33.38 salinity in the surface) shelf break waters in the marginal sea ice zone with 18-m MLD; (ii) exp. 2: relatively warmer (0.05 °C and 33.99 salinity in the surface) waters in the central polynya with 51-m MLD. In the study area, Antarctic Surface Water which is defined as the water on the continental slope and shelf where the neutral density is < 28.0 and temperature is > −1.85 °C (Orsi and Wiederwohl, 2009), was found on the entire surface layer during the 2016 cruise. At both stations, the vertical distributions of chl-a were higher in the surface layer and decreased with depth. Previously, it was reported that diatoms were dominant in shallow MLD conditions close to the ice edge, whereas *P. antarctica* was dominant in the deep MLD area in the polynya during the austral summer in the Amundsen Sea (Alderkamp et al., 2012b; Lee et al., 2016). In this study, the phytoplankton species compositions in the initial bottles showed significant differences between the two experiments (ANOSIM test, $p < 0.001$, Fig. 5), but the communities dominated by *P. antarctica* at the marginal sea ice zone, and by *P. antarctica*, *D. speculum*, and diatoms at the central polynya, indicate inconsistency with previous reports and warrant further investigation. During the incubation experiments, the average insolation was 184 $\mu Em^{-2}s^{-1}$; thus, the average light levels were 2, 55, and 92 $\mu Em^{-2}s^{-1}$ for the 1 %, 30 %, and 50 % PAR bottles, respectively (Fig. 2).

3.2. Taxon-specific growth rates

In all incubation bottles, 7 to 8 phytoplankton species were dominant in the phytoplankton abundance (>85 %) and C biomass (>85 %) during the entire incubation period; thus, the taxon-specific growth rates of these major contributors were calculated (Fig. 3a and b). Although the phytoplankton species composition in the seawater used in exp. 1 and 2 showed a significant difference (ANOSIM $R = 0.43$, $p < 0.001$, Fig. 5), the changes in the growth rate of each dominant species for light did not show a significant difference in the two experiments, indicating the species-specific consistent response of phytoplankton species to light. The growth rates of the most major species were highly dependent on increasing light intensity (ANOVA test, $p < 0.001$) but showed intra-specific variations.

Small pennates *Fragilariopsis cylindrus/curta* and *Pseudonitzschia prolongatoides/subcurvata* dramatically increased in the growth rates to about 0.40 d^{-1} under elevated light levels in both experiments, and that of *P. antarctica* also increased in a range of 0.22–0.41 d^{-1}. When comparing these three fast-growing species, diatoms appear to be able to outcompete *P. antarctica* at high light levels, which is consistent with previous studies suggesting that Antarctic diatoms showed higher levels of photo protection than *P. antarctica* when grown under high irradiance (Kropuenske et al., 2009; van de Poll et al., 2011). However, these previous studies were for one or two species that respond somewhat differently to light, and there have been warnings that it is necessary to verify these conclusions by investigating more diatom species (Mills et al., 2010). Because *P. antarctica* is one species and diatoms is a class level comprised of several species that differ in their spatial distribution according to the species in the Amundsen Sea coastal waters (Lee et al., 2016), it could be difficult to apply it to the phytoplankton community distributions in the ASP only by understanding at this class level.

In our in situ incubation experiments, the response to increasing light varied between species. Small pennates significantly increased with increasing light, followed by *P. antarctica*. The growth rate of the centric diatom *Chaetoceros* spp. was similar to that of *P. antarctica*, but those of large diatoms, *Proboscia* spp. and *Plagiotropus* spp., slightly increased in the experiment bottles and with lower growth rates than that of *P. antarctica* at high light levels, indicating that algal growth rates decrease with increasing cell size. Allometry for phytoplankton is the study of the relationship of body size to physiology and has long been conducted in research (Banse, 1976, 1982; Geider et al., 1986). The relationship between cell size and maximum specific growth rate in phytoplankton has been reported previously (Eppley and Sloan, 1966), and it was demonstrated that the growth rate of phytoplankton species is due to the size dependence of their metabolic rates (Banse, 1982), catalytic efficiencies, and light absorption (Geider et al., 1986). On the other hand, it has been reported that the correlation between growth rate and cell size is weak because the physiological characteristics of phytoplankton are different for each group and the growth rate is different depending on the life cycle of the same species (Chisholm, 1992). However, during our cruise, it was found that the growth rates of major phytoplankton species in the Amundsen Sea were size-dependent under the same environmental conditions (Fig. 3c). These results provide important information for understanding the phytoplankton community distribution in the Amundsen Sea coastal waters. Under high light conditions, some diatoms grow faster than *P. antarctica*, while others grow slower, which is consistent with previous studies that have shown inter- and intra-specific variations (Table S1). Phytoplankton distribution has been understood in previous studies based on information on fast-growing diatoms, such as *F. cylindrus*, but in the Amundsen Sea, slow-growing large-sized diatoms are also an important contributor to phytoplankton biomass, especially in the marginal sea ice zone (Lee et al., 2016). To date, the nature of these large diatoms is poorly characterized, even though they play an important role in C export. Thus, further investigation of this group is warranted to understand the phytoplankton dynamics in the Amundsen Sea.

3.3. Phytoplankton composition, abundance, and C biomass

At the end of the incubations, phytoplankton abundance and biomass dramatically increased in all incubation bottles except for the 1 % PAR bottles, while the changes in the dominant rate of each species differed between the abundance and biomass results (Fig. 4). The dominant rate of small pennates in the phytoplankton abundance and biomass

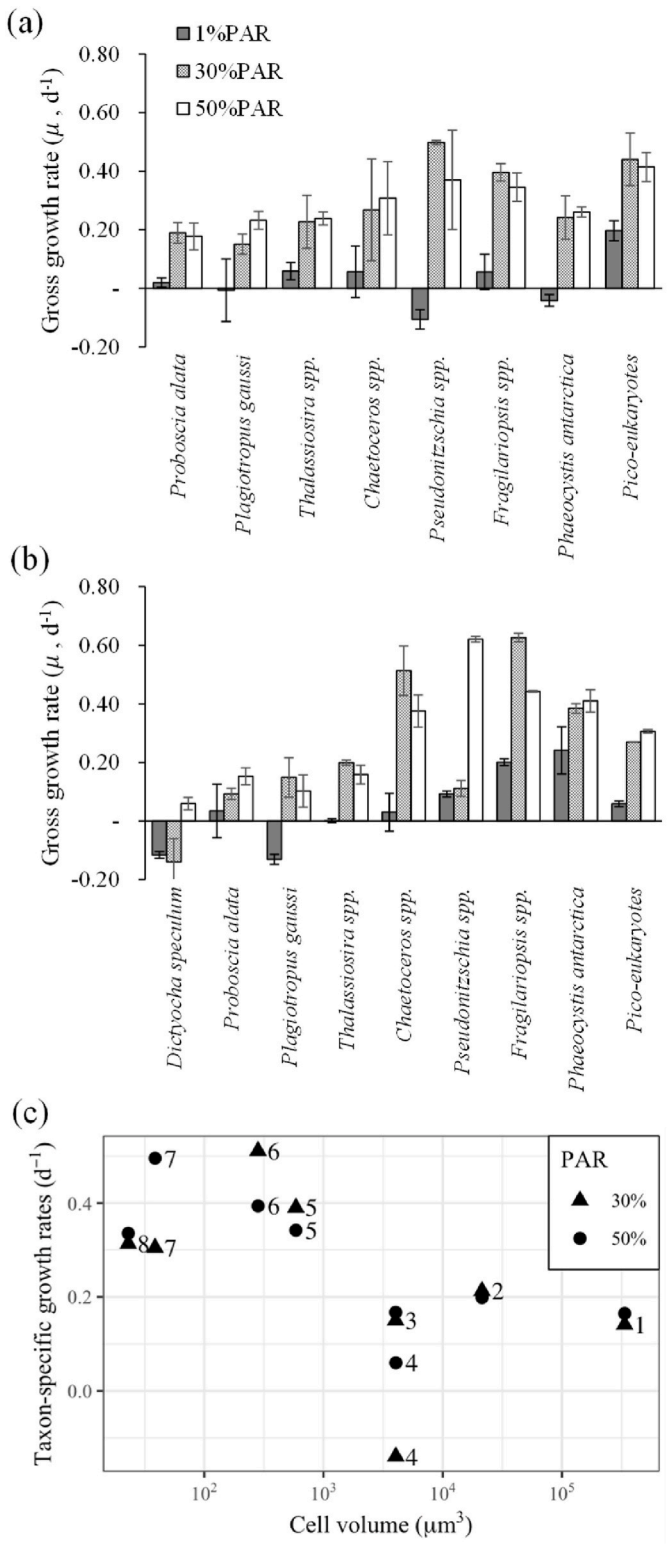

Fig. 3. Average taxon-specific growth rates (μ, d^{-1}) and standard deviation (error bar) for major phytoplankton species observed in (a) experiment 1 and (b) 2 on natural populations. (c) Relationship between cell volume and the taxon-specific growth rates of major phytoplankton species under different light levels. The algae are: 1, *Proboscia alata*; 2, *Thalassiosira* spp.; 3, *Plagiotropus gaussi*; 4, *Dictyocha speculum*; 5, *Chaetoceros* spp.; 6, *Fragilariopsis cylindrus/curta*; 7, *Pseudonitzschia prolongatoides/subcurvata*; 8, *Phaeocystis antarctica*.

exhibited the highest rate of increase at high light levels, while *P. antarctica* slightly increased their dominant rates with a decrease in the dominance of large diatoms and *D. speculum* in the phytoplankton C biomass. Phytoplankton cell size ranged over three orders of magnitude: from <2 μm up to 2000 μm (Beardall et al., 2009). Thus, cells of different sizes contribute differently to the phytoplankton C biomass due to the size dependence of cellular C as a function of cell volume. Changes in the dominant rate of the phytoplankton species in terms of their abundance and C biomass were complicated at the end of the incubations.

First, different initial compositions of phytoplankton species would affect the phytoplankton community composition after incubation. The phytoplankton composition in the natural communities used in each experiment was different between stations. At station four, *P. antarctica* dominated with a relative abundance of 92 %, followed by diatoms (7 %), while *P. antarctica*, *D. speculum*, and diatoms accounted for 47 %, 20 %, and 18 % of the phytoplankton abundance, respectively, at station 12. Meanwhile, diatoms accounted for 76 % and 46 % of the phytoplankton C biomass at stations 4 and 12, respectively, because of their larger size and higher C content compared to *P. antarctica* (relative C biomasses of 23 % and 1 % at stations 4 and 12, respectively). The major diatoms observed in both stations were *Fragilariopsis cylindrus/curta*, *Pseudonitzschia prolongatoides/subcurvata*, *Chaetoceros* spp., *Thalassiosira* spp., *Plagiotropus gaussi*, and *Proboscia alata*. NMDS analysis based on the Bray-Curtis dissimilarity for the log-transformed phytoplankton species abundance also showed that the samples grouped together according to the experiments (Fig. 5). In all incubation bottles, significant differences in phytoplankton community composition were identified between the experiments (ANOSIM $R = 0.43$, $p < 0.001$), indicating the effect of the initial species composition of phytoplankton on their community structure after incubation.

Second, at the elevated light levels, the dominant rate of each species changed differently from the initial rate due to the differences in the response of each species to light. The dominant rate of *P. antarctica* and small pennates significantly increased in phytoplankton biomass as a consequence of their highest growth rates among the phytoplankton species in the incubation bottles. Centric diatoms *Chaetoceros* and *Thalassiosira* and large diatom *Proboscia* all grew; however, their dominant rates in the phytoplankton abundance and biomass decreased at the end of the incubations due to a relatively slower growth rate than those of the small size species. *D. speculum* was a dominant species in the seawater at station 12, but their abundance in all incubation bottles decreased compared to the start of the experiment, except for the 50 % PAR bottles. The ecology and physiology of the chrysophyte *D. speculum* in Antarctic coastal waters are practically unknown, but it has been reported that this species favors the shallow MLD of the Ross Sea and the ASP (Fragoso and Smith Jr, 2012). More information is required to understand the ecological characteristics of this species.

Finally, variations between species as well as within species were observed. The cell size of *P. antarctica* increased dramatically in all bottles. *P. antarctica* has polymorphic life cycles that include colonial cells (3.2–10 μm in size) in the spherical colony and two types of flagellates (Rousseau et al., 2007). Small flagellates of *P. antarctica* (3.5–7 μm) were shown to be mostly present before colony blooms, and it appears that the light level and turbulence would play a key role in colony generation from flagellates (Peperzak, 1993; Schapira et al., 2006). Thus, it is likely that the increase in irradiance, the maintenance of a constant amount of light, and the stable environment in the incubation bottles with weak mixing compared to the ocean might be important factors for the increase in the cell size of *P. antarctica*. The C biomass of *P. antarctica* is estimated using the conversion factor of C per cell. However, the size of flagellate cells can affect the C biomass, so if this is reflected in the C biomass, the dominant rate of *P. antarctica* may increase more than this result. Diatom species showed no significant change in cell size during the 9-day incubation period.

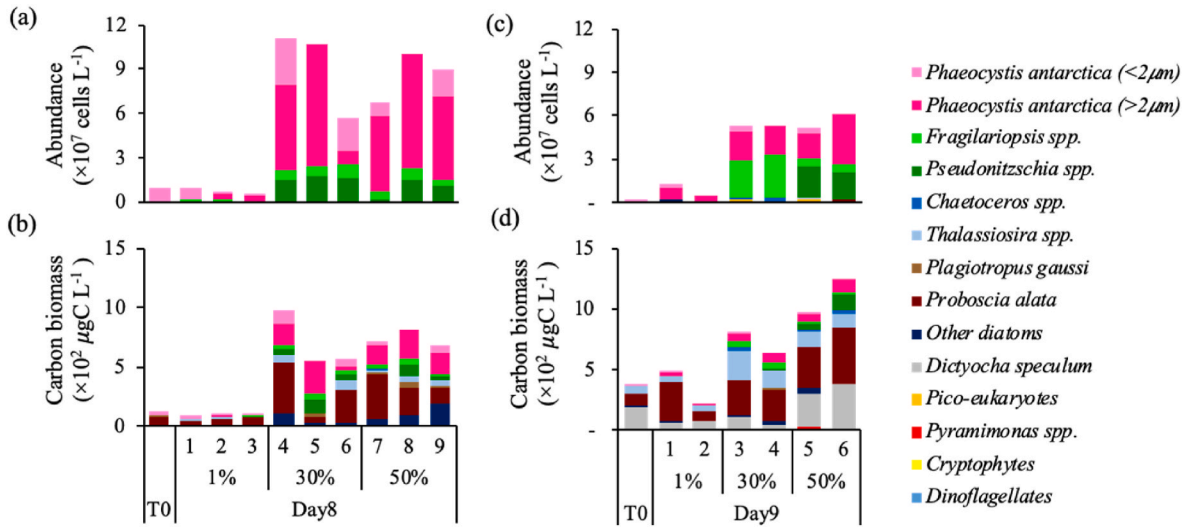

Fig. 4. (a, c) Abundance (cellsL^{-1}) and (b, d) carbon biomass (μgCL^{-1}) of the major phytoplankton species and minor groups in the initial and the final days of the incubations under different light treatments for experiment 1 (a, b) and 2 (c, d).

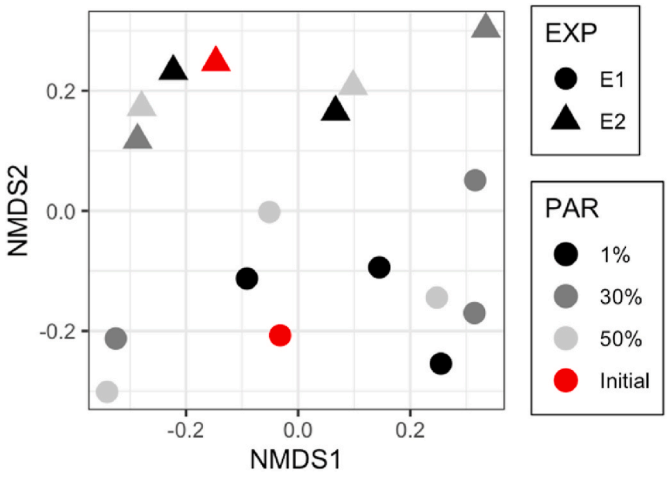

Fig. 5. Non-metric multidimensional scaling (NMDS) analysis based on Bray-Curtis dissimilarities of the phytoplankton species abundance in each incubation bottle for the experiments (Stress value = 0.171). The red and grayscale figures indicate the samples in the initial and final days of the incubations, respectively. (For interpretation of the references to color in this figure legend, the reader is referred to the Web version of this article.)

3.4. Nutrient uptake and pigment content

The concentrations of macronutrients, including dissolved inorganic nitrogen (DIN),[16] P, and Si in the surface seawater were more than 22 μM, 1.6 μM, and 77 μM, respectively, indicating nutrient replete in the sampling stations (Table 1). At the end of the incubations, the nutrient concentrations in the 30 % and 50 % PAR bottles decreased significantly except for ammonia in the two experiments. Ammonium is one of the major forms of bound nitrogen available to phytoplankton, and its relative amount depends on chemical processes such as redox transformations, as well as biological processes such as the bacterial degradation of organic nitrogen compounds and differential utilization by phytoplankton groups (Bianchi et al., 1997; Domingues et al., 2011). At the end of the incubations, the ammonia concentrations showed a higher rate of increase in exp. 2 than in exp. 1 with a large increase in 30 % PAR bottles compared to 50 %, which probably indicates differences in the preference and uptake rate of ammonia according to the phytoplankton community structure and biomass in each incubation bottle. The NOx concentrations in the 50 % PAR bottles were below the detection limit, indicating a relatively higher uptake rate of nitrate by the phytoplankton at high light levels after 8–9 days of incubations. As a high nutrient low chlorophyll ecosystem, the Southern Ocean is characterized by high nitrate concentrations (Boyd et al., 2007; de Baar et al., 1990), thus nitrate depletion has very rarely been reported in large phytoplankton blooms in the west Antarctic Peninsula region and the Ross Sea (Ducklow et al., 2007; Fitzwater et al., 2000), indicating that it rarely appears as a major limiting factor for phytoplankton growth, unlike light and iron. The bottles were incubated until the nitrate was depleted, and by not adding additional nitrate to the bottles, a self-shading of high phytoplankton biomass was minimized.

During the incubations, the nutrient concentrations showed a significant decrease, but the drawdown of each nutrient were slightly different between experiments. Since the NOx concentrations in some bottles were below the detection limit on the final days of both incubations, the nutrient concentrations on day 6 were used to calculate the nutrient drawdown and nutrient ratio (Table 1). At the increased light levels, the P drawdown from the initial values ranged from 0.71 μM to 0.93 μM in all incubation bottles on day 6. The NOx drawdown in 50 % PAR bottles was higher (18.8 μM and 18.0 μM in exp.1 and exp.2, respectively) than that in 30 % PAR bottles (14.8 μM and 15.0 μM in exp.1 and exp.2, respectively), showing no significant difference between experiments. On the contrary, the NOx:P ratios and Si drawdown slightly differed between exp. 1 and exp. 2. In 50 % PAR bottles, the difference in NOx:P ratios between the initials and the 6 day were slightly greater in exp. 1 (13.05 and 3.91, respectively) than in exp.2 (13.22 and 4.55, respectively). Diatoms and *P. antarctica* play different roles in the biogeochemical cycle of the west Antarctic coastal waters. Previous study showed that nitrogen demand was higher in the *P. antarctica* overwhelmingly dominated region (>90 % of total phytoplankton biomass) than in the diatoms dominated region (>85 %) in the Ross Sea (Arrigo et al., 1999). In the increased light levels, Si drawdown was higher in exp. 2 (16.7–22.1 μM) than in exp. 1 (13.8–14.9 μM). Diatoms and silicoflagellates, such as *D. speculum*, require silicates for growth because they build their biomineralized cell walls from this material (Treguer et al., 1995). Thus, our results indicate that the drawdown of NOx and Si could be influenced by the slight difference in the dominant rates of *P. antarctica* (32 % and 9–10 % of phytoplankton C biomass in exp. 1 and exp. 2, respectively), diatoms (68 % and 60–79 %),

[16] DIN: Dissolved inorganic nitrogen.

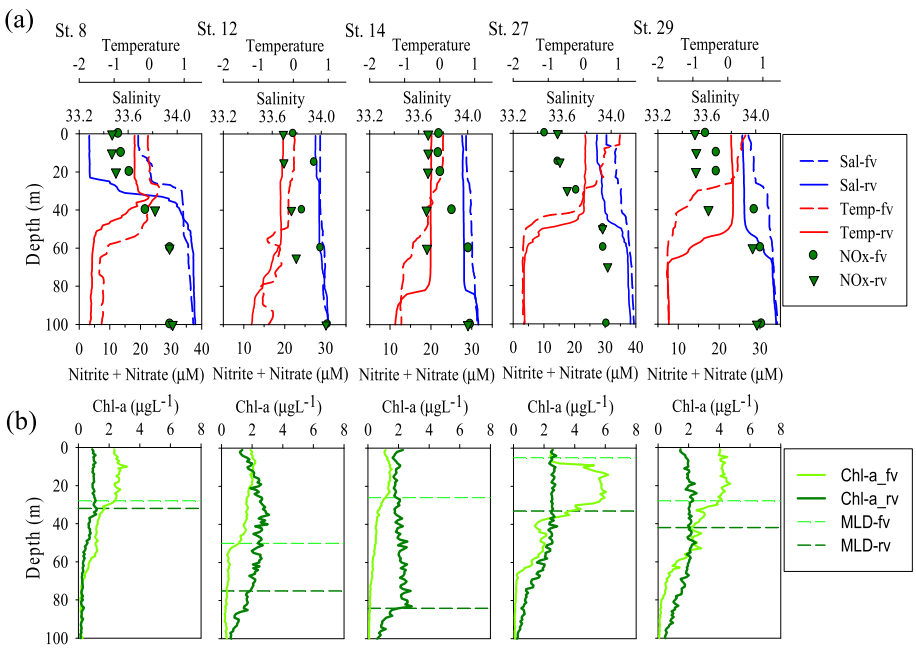

Fig. 6. Short-term variations of (a) environmental variables such as seawater temperature, salinity, nitrite + nitrate concentration, (b) MLD and phytoplankton properties such as chl-a profiles between the first visit (fv) and the revisit (rv) in the ASP. Chl-a profiles were calibrated using chlorophyll fluorescence with the extracted chl-a concentration of the discrete water samples. Sal, salinity; Temp, temperature; NOx, nitrite + nitrate; MLD, mixed layer depth.

and *D. speculum* (Not detected in exp. 1 and 8–30 % in exp. 2) at the high light levels on the final days of the incubations.

In the seawater used in the bioassay experiments, hex-fuco and fuco showed high concentrations of the photosynthetic pigments, indicating that *P. antarctica* and diatoms were the dominant group in the phytoplankton biomass (Table 1). At the final days of the incubations, chl-a concentrations in the 1 % PAR bottles were similar to the initial values, but it dramatically increased by more than 2.2 times in the 30 % and 50 % PAR bottles, showing high phytoplankton growth at the elevated light levels. Unlike chl-a, each pigment concentration changed differently in the two experiments after the incubation. Hex-fuco per chl-a was significantly increased at high light intensity only in exp. 1, while accessary pigments per chl-a were not significantly different between all bottles in experiment 2. In the 50 % PAR bottles, photoprotective pigments (DD, DT) normalizing to chl-a (Higgins et al., 2011) increased from 0.10 at the initial days to 0.34 at the final days in the exp. 1, while it was similar to the initial value in exp. 2 (0.24 and 0.20 at the initial and the final days, respectively). Previous photophysiological studies reported that *P. antarctica* is better adapted to grow than *F. cylindrus* in a dynamic light environment, typical for a deep MLD by changing their cellular pigment contents (Kropuenske et al., 2009; van de Poll et al., 2011). Bulk community measurements using in situ sea water do not provide information on the response of individual species, such as elemental ratios and pigment contents; however, these results imply that the photophysiological response of *P. antarctica* might be reflected in the incubation bottles of exp. 1 due to the dominant rate of *P. antarctica* in the phytoplankton biomass being relatively higher in exp. 1.

3.5. Effect of short-term environmental changes on phytoplankton distribution

Compared to mid-January, the environmental variables in the surface layer have changed to a lower seawater temperature, lower salinity, lower nitrate concentrations, deeper MLD, and a higher light insolation at the revisit stations of the ASP in early February (Figs. 2 and 6). Compared to the first visit in January, *P. antarctica* and small pennates, *Fragilariopsis* spp., *Pseudonitzschia* spp., and *Cylindrotheca closterium*, increased in abundance in the surface layer during the revisit (Figs. 7 and 8). In the ASP, phytoplankton bloom generally peaked within a week or two of mid-January, and then decline steadily and terminated on the end of February probably due to the limiting factors such as iron, solar radiation, or grazing pressure (Arrigo et al., 2012; Mills et al., 2012; Yang et al., 2019). However, phytoplankton abundance was higher in early February than mid-January in the ASP during this study.

NMDS analysis based on Bray-Curtis dissimilarity for log-transformed phytoplankton species abundance showed that the samples group together according to their sampling date except station 14 (Fig. 9), with most dissimilarity due to changes in the abundance of *Proboscia alata* (Indicator species analysis, $p < 0.01$), *Dictyocha speculum* ($p < 0.01$), and *Thalassiosira* spp. ($p < 0.05$) between the first visit and revisit. When available environmental variables were fitted against the NMDS analysis, a higher nutrient concentration and salinity were associated with the first visit, while a deeper euphotic depth and higher PAR (3 day average PAR prior to the sampling periods at the individual stations) were associated with the revisit. A slight decrease in nitrate concentration in the surface layer during the revisit (Fig. 6a) indicates nutrient uptake and the growth of phytoplankton. These results could imply that iron, which is an important limiting factor for phytoplankton growth in Antarctic coastal waters during the post-bloom period (Alderkamp et al., 2015; de Baar et al., 1990), might not have been the major controller for phytoplankton growth during the study period. Otherwise, iron might be supplied from deeper waters to the surface due to the deeper MLD during the revisit. Average solar radiation was higher during the revisit (243 ± 259 $\mu Em^{-2}s^{-1}$) than the first visit (193 ± 180 $\mu Em^{-2}s^{-1}$), and small phytoplankton dramatically increased in their abundance in the surface layer during revisit, showing consistency with our incubation experiments. Grazing pressure at higher trophic levels may be one of the important limiting factors for phytoplankton biomass during the revisit. However it has been previously reported that microzooplankton herbivory may not contribute significantly to the decline of the phytoplankton bloom, and mesozooplankton does not effectively feed on diatoms and *P. antarctica* in the ASP (Yang et al., 2019). Thus, it is more likely that the growth of phytoplankton species may be regulated by light availability in the ASP during the austral summer of 2016.

Interestingly, the surface chl-a concentration decreased during the

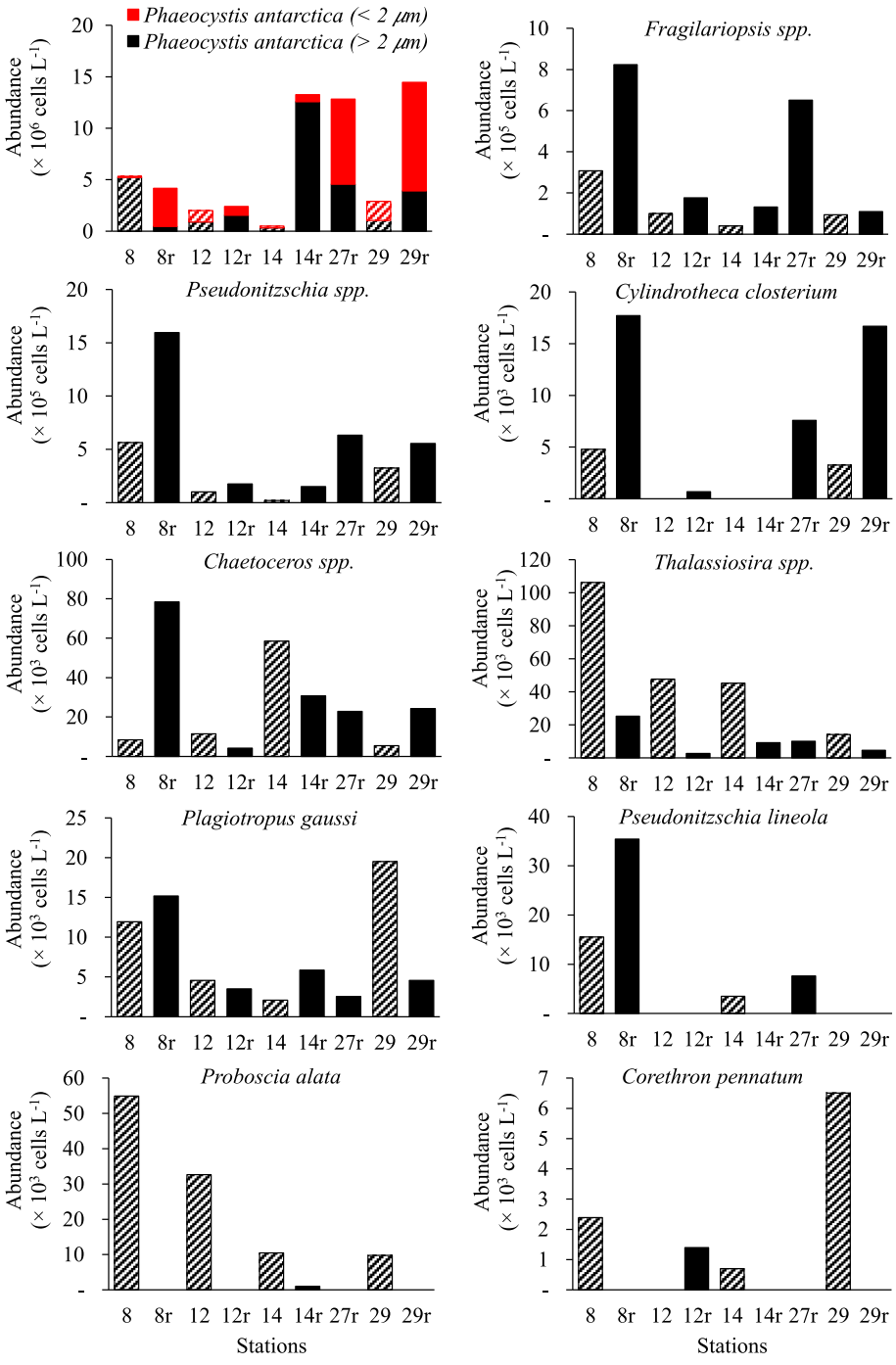

Fig. 7. Comparison of the abundance of major phytoplankton species in the surface layer at each station of the Amundsen Sea coastal area between the first visit (mid-January) and the revisit (early February) in 2016. The "r" after the station number indicates the revisit.

revisit (Fig. 6b) even though there was an increase in the abundance of phytoplankton. During the first visit, large diatoms were a major contributor to the phytoplankton C biomass in the surface layer (Fig. 8), and the lower chl-a concentration during the revisit was caused by the decrease in abundance of this group (Fig. 7). In the previous research, it was suggested that phytoplankton distribution could be influenced by the size and buoyance of each species because larger phytoplankton with lower surface area-to-volume ratios have the disadvantage of higher sinking rates after seeding from sea ice in spring (Garrison et al., 2003; Kang and Fryxell, 1992; Lee et al., 2016). Unlike small-sized species, the decrease in abundance of large diatoms in the surface layer during the revisit could be assumed to be due to their high settling rate (Lee et al., 2016) and low growth rate (this study), but further investigation is warranted. These results imply that information about phytoplankton species composition provides a deeper understanding of phytoplankton ecology in the Antarctic coast. If we tried to understand our results based only on the chl-a concentration, it could be assumed that these results represent a seasonal change in which the surface phytoplankton biomass decreases due to limiting factors such as iron and light, changing from the bloom period in January to the post-bloom period in February. However, each phytoplankton group had different ecological and physiological properties in the ASP during this study. Large diatoms are important contributors to C sequestration in the ASP (Kim et al., 2015), and small pennates could be a major food source in the pelagic food web

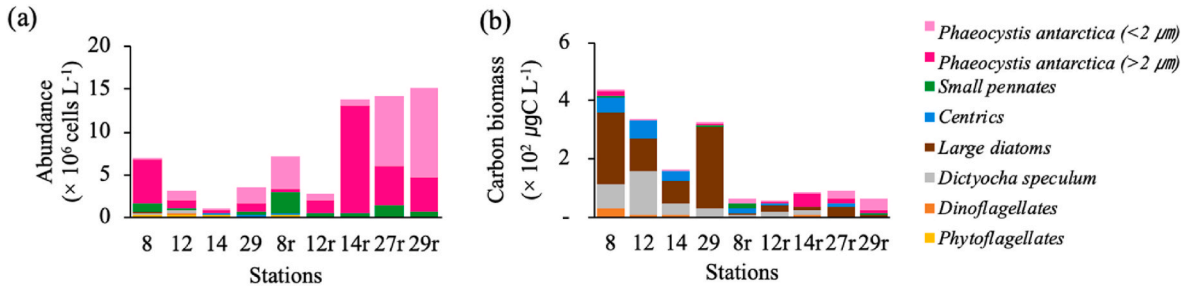

Fig. 8. Short-term variations (a) abundance and (b) carbon biomass of phytoplankton groups between the first visit and the revisit in the surface layer of the ASP. The "r" after the station number indicates the revisit.

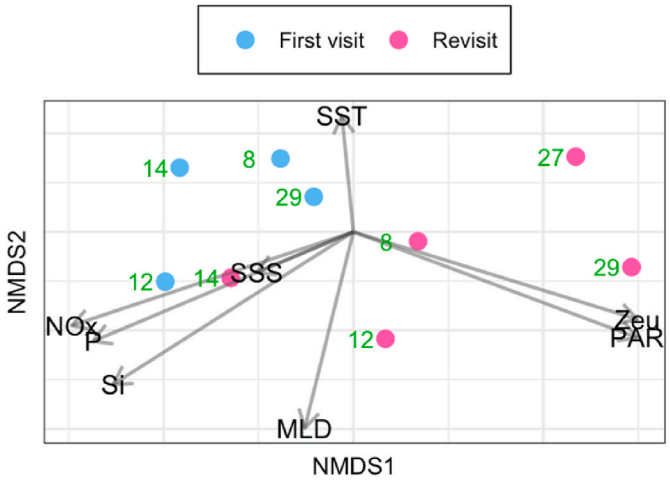

Fig. 9. Two-dimensional non-metric multidimensional scaling (NMDS) ordination plots based on Bray-Curtis dissimilarities of the phytoplankton community composition (log-transformed species abundance) during the first visit and revisit (Stress value = 0.097). The arrow length and direction depict the strength and nature of the relationships. The green number indicates the station. SST, sea surface temperature; SSS, sea surface salinity; NOx, nitrite + nitrate; P, phosphate; Si, silicate; MLD, mixed layer depth; Zeu, euphotic depth; PAR, photosynthetically active radiation. (For interpretation of the references to color in this figure legend, the reader is referred to the Web version of this article.)

(Yang et al., 2019). Thus, more field studies based on species information should be performed to estimate the response of various phytoplankton in the rapidly changing ASP.

4. Conclusions

During the austral summer in 2016, the distribution of the phytoplankton community in the ASP was likely to be limited by low irradiance. In the incubation experiments, small pennates grew rapidly, followed by *P. antarctica*, centric diatoms, and large diatoms when the light increased, which most likely indicates changes in the community and size structures of the phytoplankton under various light conditions in the water column. The dominant rates of the small pennates and *P. antarctica* in the phytoplankton abundance and biomass dramatically increased at elevated light levels after 8–9 d of incubation compared to the initial levels. Large diatoms showed low growth and dominant rates at the end of the incubations, but still accounted for approximately 50 % of the phytoplankton biomass owing to their larger size and higher C content. A short-term study also showed that light could be the major controller of phytoplankton species distribution. Environmental changes in basal melting, sea ice concentration, water column stratification, and cloud concentration caused by global warming are altering the underwater light properties. Phytoplankton community composition and biomass could be affected by the variability in light intensity according to our results, and consequently may regulate food web structures due to the size dependence of prey selection in zooplankton and the negative effects of *P. antarctica* on zooplankton (Gasparini et al., 2000; Nejstgaard et al., 2007; Yang et al., 2019). Meanwhile, phytoplankton communities are comprise various diatoms in the ASP. Therefore, the use of the physiological characteristics of one or two diatom species to understand the distributions of the entire group of diatoms might lead to a hasty generalization error. Thus, in situ incubation experiments on phytoplankton communities should be considered in addition to autecological studies in the laboratory in order to understand and predict the phytoplankton distribution in the rapidly changing Antarctic coastal waters.

Credit author statement

Youngju Lee: Conceptualization, Methodology, Validation, Formal analysis, Investigation, Writing – original draft, Writing – review & editing, Visualization. Jinyoung Jung: Investigation, Writing – review & editing, Tae Wan Kim: Investigation, Writing – review & editing. Eun Jin Yang: Writing – review & editing. Jisoo Park: Writing – review & editing, Project administration.

Funding statement

Funding for this research was obtained from the Korea Polar Research Institute (KOPRI) (PE21110).

Declaration of competing interest

The authors declare that they have no known competing financial interests or personal relationships that could have appeared to influence the work reported in this paper.

Acknowledgements

The authors thank the captain and crew of the *IBRV* ARAON who were most helpful in all shipboard operations. We gratefully acknowledge the anonymous reviewers for their constructive and insightful comments.

Appendix A. Supplementary data

Supplementary data to this article can be found online at https://doi.org/10.1016/j.envres.2021.112165.

References

Alderkamp, A.-C., Kulk, G., Buma, A.G., Visser, R.J., Van Dijken, G.L., Mills, M.M., Arrigo, K.R., 2012a. The effect of iron limitation of the photophysiology of *Phaeocystis antarctica* (Prymnesiophyceae) and *Fragilariopsis cylindrus* (Bacillariophyceae) under dynamic irradiance. J. Phycol. 48, 45–59.
Alderkamp, A.-C., Mills, M.M., van Dijken, G.L., Laan, P., Thuróczy, C.E., Gerringa, L.J. A., de Baar, H.J.W., Payne, C.D., Visser, R.J.W., Buma, A.G.J., Arrigo, K.R., 2012b.

Iron from melting glaciers fuels phytoplankton blooms in the Amundsen Sea (Southern Ocean): phytoplankton characteristics and productivity. Deep-Sea Res. PT II 71–76, 32–48.
Alderkamp, A.-C., van Dijken, G.L., Lowry, K.E., Connelly, T.L., Lagerström, M., Sherrell, R.M., Haskins, C., Rogalsky, E., Schofield, O., Stammerjohn, S.E., 2015. Fe availability drives phytoplankton photosynthesis rates during spring bloom in the Amundsen Sea Polynya, Antarctica. Elem. Sci. Anthr. 3, 000043.
Arrigo, K.R., Brown, Z.W., Mills, M.M., 2014. Sea ice algal biomass and physiology in the Amundsen Sea, Antarctica. Elem. Sci. Anthr. 2, 000028.
Arrigo, K.R., Lowry, K.E., van Dijken, G.L., 2012. Annual changes in sea ice and phytoplankton in polynyas of the Amundsen Sea, Antarctica. Deep-Sea Res. PT II 71, 5–15.
Arrigo, K.R., Robinson, D.H., Worthen, D.L., Dunbar, R.B., DiTullio, G.R., VanWoert, M., Lizotte, M.P., 1999. Phytoplankton community structure and the drawdown of nutrients and CO_2 in the Southern Ocean. Science 283, 365–367.
Arrigo, K.R., van Dijken, G.L., 2003. Phytoplankton dynamics within 37 Antarctic coastal polynya systems. J. Geophys. Res.-Oceans. 108.
Banse, K., 1976. Rates of growth, respiration and photosynthesis of unicellular algae as realted to cell size-A review. J. Phycol. 12, 135–140.
Banse, K., 1982. Cell volumes, maximal growth rates of unicellular algae and ciliates, and the role of ciliates in the marine pelagial. Limnol. Oceanogr. 27, 1059–1071.
Beardall, J., Allen, D., Bragg, J., Finkel, Z.V., Flynn, K.J., Quigg, A., Rees, T.A.V., Richardson, A., Raven, J.A., 2009. Allometry and stoichiometry of unicellular, colonial and multicellular phytoplankton. New Phytol. 181, 295–309.
Bianchi, M., Feliatra, F., Tréguer, P., Vincendeau, M.-A., Morvan, J., 1997. Nitrification rates, ammonium and nitrate distribution in upper layers of the water column and in sediments of the Indian sector of the Southern Ocean. Deep-Sea Res. PT II 44, 1017–1032.
Boyd, P.W., Jickells, T., Law, C., Blain, S., Boyle, E., Buesseler, K., Coale, K., Cullen, J., De Baar, H., Follows, M., 2007. Mesoscale iron enrichment experiments 1993-2005: synthesis and future directions. Science 315, 612–617.
Carvalho, F., Kohut, J., Oliver, M.J., Schofield, O., 2017. Defining the ecologically relevant mixed-layer depth for Antarctica's coastal seas. Geophys. Res. Lett. 44, 338–345.
Chisholm, S.W., 1992. Phytoplankton size. In: Falkowski, P.G., Woodhead, A.D. (Eds.), Primary Productivity and Biogeochemical Cycles in the Sea. Springer, New York and London, pp. 213–237.
de Baar, H., Buma, A., Nolting, R.F., Cadee, G.C., Jacques, G., Treguer, P.J., 1990. On iron limitation of the Southern Ocean: experimental observations in the weddell and Scotia seas. Mar. Ecol. Prog. Ser. 65, 105–122.
Domingues, R.B., Barbosa, A.B., Sommer, U., Galvão, H.M., 2011. Ammonium, nitrate and phytoplankton interactions in a freshwater tidal estuarine zone: potential effects of cultural eutrophication. Aquat. Sci. 73, 331–343.
Dotto, T.S., Naveira Garabato, A.C., Wåhlin, A.K., Bacon, S., Holland, P.R., Kimura, S., Tsamados, M., Herraiz-Borreguero, L., Kalén, O., Jenkins, A., 2020. Control of the oceanic heat content of the Getz-Dotson trough, Antarctica, by the Amundsen Sea low. J. Geophys. Res.-Oceans. 125, e2020JC016113.
Ducklow, H.W., Baker, K., Martinson, D.G., Quetin, L.B., Ross, R.M., Smith, R.C., Stammerjohn, S.E., Vernet, M., Fraser, W., 2007. Marine pelagic ecosystems: the west Antarctic Peninsula. Phil. Trans. Biol. Sci. 362, 67–94.
Eppley, R.W., Sloan, P.R., 1966. Growth rates of marine phytoplankton: correlation with light absorption by cell chlorophyll *a*. Physiol. Plantarum 19, 47–59.
Fitzwater, S., Johnson, K., Gordon, R., Coale, K., Smith Jr., W., 2000. Trace metal concentrations in the Ross Sea and their relationship with nutrients and phytoplankton growth. Deep-Sea Res. PT II. 47, 3159–3179.
Fragoso, G.M., Smith Jr., W.O., 2012. Influence of hydrography on phytoplankton distribution in the Amundsen and Ross seas, Antarctica. J. Mar. Syst. 89, 19–29.
Garrison, D.L., Gibson, A., Kunze, H., Gowing, M.M., Vickers, C.L., Mathot, S., Bayre, R. C., 2003. The Ross Sea polynya Project: diatom- and *Phaeocystis*-dominated phytoplankton assemblages in the Ross Sea, Antarctica, 1994–1996. In: DiTullio, G. R., Dunbar, R.B. (Eds.), Biogeochemistry of the Ross Sea Antarctic Research. American Geophysical Union, Washington D. C., pp. 53–76
Gasparini, S., Daro, M.H., Antajan, E., Tackx, M., Rousseau, V., Parent, J.-Y., Lancelot, C., 2000. Mesozooplankton grazing during the *Phaeocystis globosa* bloom in the southern bight of the North Sea. J. Sea Res. 43, 345–356.
Geider, R.J., Platt, T., Raven, J.A., 1986. Size dependence of growth and photosynthesis in diatoms: a synthesis. Mar. Ecol. Prog. Ser. 30, 93–104.
Gerringa, L.J.A., Alderkamp, A.C., Laan, P., Thuróczy, C.E., De Baar, H.J.W., Mills, M.M., van Dijken, G.L., Haren, H.V., Arrigo, K.R., 2012. Iron from melting glaciers fuels the phytoplankton blooms in Amundsen Sea (Southern Ocean): iron biogeochemistry. Deep-Sea Res. PT II 71–76, 16–31.
Higgins, H.W., Wright, S.W., Schluter, L., 2011. Quantitative interpretation of chemotaxonomic pigment data. In: Roy, S., Llewellyn, C.A., Egeland, E.S., Johnsen, G. (Eds.), Phytoplankton Pigments: Characterization, Chemotaxonomy and Applications in Oceanography. Cambridge University Press, United Kingdom, pp. 257–313.
Hillebrand, H., Dürselen, C.D., Kirschtel, D., Pollingher, U., Zohary, T., 1999. Biovolume calculation for pelagic and benthic microalgae. J. Phycol. 35, 403–424.
Holland, M.M., Landrum, L., Raphael, M.N., Kwok, R., 2018. The regional, seasonal, and lagged influence of the Amundsen Sea Low on Antarctic sea ice. Geophys. Res. Lett. 45, 11,227–11,234.
Jeffrey, S., Mantoura, R., Wright, S. (Eds.), 1997. Phytoplankton Pigments in Oceanography: Guidelines to Modern Methods. Unesco, Paris, 661.
Kang, S.-H., Fryxell, G.A., 1992. *Fragilariopsis cylindrus* (Grunow) Krieger: the most abundant diatom in water column assemblages of Antarctic marginal ice-edge zones. Polar Biol. 12, 609–627.
Kim, M., Hwang, J., Kim, H.J., Kim, D., Yang, E.J., Ducklow, H.W., La Hyoung, S., Lee, S. H., Park, J., Lee, S., 2015. Sinking particle flux in the sea ice zone of the Amundsen shelf, Antarctica. Deep-Sea Res. PT I. 101, 110–117.
Kropuenske, L.R., Mills, M.M., van Dijken, G.L., Bailey, S., Robinson, D.H., Welschmeyer, N.A., Arrigo, K.R., 2009. Photophysiology in two major Southern Ocean phytoplankton taxa: photoprotection in *Phaeocystis antarctica* and *Fragilariopsis cylindrus*. Limnol. Oceanogr. 54, 1176.
Lee, Y., Yang, E.J., Park, J., Jung, J., Kim, T.W., Lee, S., 2016. Physical-biological coupling in the Amundsen Sea, Antarctica: influence of physical factors on phytoplankton community structure and biomass. Deep-Sea Res. PT I. 117, 51–60.
Mathot, S., Smith, W.O., Carlson, C.A., Garrison, D.L., Gowing, M.M., Vickers, C.L., 2000. Carbon partitioning within *Phaeocystis antarctica* (Prymnesiophyceae) colonies in the Ross Sea, Antarctica. J. Phycol. 36, 1049–1056.
Mills, M.M., Alderkamp, A.-C., Thuroczy, C.-E., van Dijken, G.L., Laan, P., de Baar, H.J. W., Arrigo, K.R., 2012. Phytoplankton biomass and pigment responses to Fe amendments in the Pine Island and Amundsen polynyas. Deep-Sea Res. PT II 71–76, 61–76.
Mills, M.M., Kropuenske, L.R., van Dijken, G.L., Alderkamp, A.-C., Berg, G.M., Robinson, D.H., Welschmeyer, N.A., Arrigo, K.R., 2010. Photophysiology in two Southern Ocean phytoplankton taxa: photosynthesis of *Phaeocystis antarctica* (Prymnesiophyceae) and *Fragilariopsis cylindrus* (Bacillariopyceae) under simulated mixed-layer irradiance. J. Phycol. 46, 1114–1127.
Nejstgaard, J.C., Tang, K.W., Steinke, M., Dutz, J., Koski, M., Antajan, E., Long, J.D., 2007. Zooplankton grazing on *Phaeocystis:* a quantitative review and future challenges. Biogeochemistry 83, 147–172.
Oliver, H., St-Laurent, P., Sherrell, R.M., Yager, P.L., 2019. Modeling iron and light controls on the summer *Phaeocystis antarctica* bloom in the Amundsen Sea Polynya. Global Biogeochem. Cycles 33, 570–596.
Orsi, A.H., Wiederwohl, C.L., 2009. A recount of Ross Sea waters. Deep-Sea Res. PT II 56, 778–795.
Pan, B., Vernet, M., Reynolds, R., Mitchell, B., 2019. The optical and biological properties of glacial meltwater in an Antarctic fjord. PLoS One 14, e0211107.
Park, J., Kuzminov, F.I., Bailleul, B., Yang, E.J., Lee, S., Falkowski, P.G., Gorbunov, M.Y., 2017. Light availability rather than Fe controls the magnitude of massive phytoplankton bloom in the Amundsen Sea polynyas, Antarctica. Limnol. Oceanogr. 62, 2260–2276.
Parsons, T., Maita, Y., Lalli, C. (Eds.), 1984. A Manual of Chemical and Biological Methods for Seawater Analysis. Pergamon Press, Oxford, pp. 101–112.
Peperzak, L., 1993. Daily irradiance governs growth rate and colony formation of *Phaeocystis* (Prymnesiophyceae). J. Plankton Res. 15, 809–821.
Raphael, M.N., Marshall, G., Turner, J., Fogt, R., Schneider, D., Dixon, D., Hosking, J., Jones, J., Hobbs, W.R., 2016. The Amundsen sea low: variability, change, and impact on Antarctic climate. Bull. Am. Meteorol. Soc. 97, 111–121.
Rignot, E., Jacobs, S., Mouginot, J., Scheuchl, B., 2013. Ice-shelf melting around Antarctica. Science 341, 266–270.
Rousseau, V., Chrétiennot-Dinet, M.-J., Jacobsen, A., Verity, P., Whipple, S., 2007. The life cycle of *Phaeocystis*: state of knowledge and presumptive role in ecology. Biogeochemistry 83, 29–47.
Rynearson, T.A., Armbrust, E.V., 2004. Genetic differentiation among populations of the planktonic marine diatom *Ditylum brightwellii* (Bacillariophyceae). J. Phycol. 40, 34–43.
Samuel, R.L., Richard, A.K., John, M.T., 2017. The euphotic zone under Arctic Ocean sea ice: vertical extents and seasonal trends. Limnol. Oceanogr. 62, 1910–1934.
Schapira, M., Seuront, L., Gentilhomme, V., 2006. Effects of small-scale turbulence on *Phaeocystis globosa* (Prymnesiophyceae) growth and life cycle. J. Exp. Mar. Biol. Ecol. 335, 27–38.
Silvano, A., Rintoul, S.R., Peña-Molino, B., Hobbs, W.R., van Wijk, E., Aoki, S., Tamura, T., Williams, G.D., 2018. Freshening by glacial meltwater enhances melting of ice shelves and reduces formation of Antarctic Bottom Water. Sci. Adv. 4, eaap9467.
Smayda, T.J. (Ed.), 1978. From Phytoplankters to Biomass. UNESCO, Paris, pp. 273–279.
Strzepek, R.F., Harrison, P.J., 2004. Photosynthetic architecture differs in coastal and oceanic diatoms. Nature 431, 689–692.
Taylor, A.G., Landry, M.R., Selph, K.E., Yang, E.J., 2011. Biomass, size structure and depth distributions of the microbial community in the eastern equatorial Pacific. Deep-Sea Res. PT II 58, 342–357.
Treguer, P., Nelson, D.M., Van Bennekom, A.J., DeMaster, D.J., Leynaert, A., Queguiner, B., 1995. The silica balance in the world ocean: a reestimate. Science 268, 375–379.
van de Poll, W.H., Lagunas, M., de Vries, T., Visser, R.J., Buma, A.G., 2011. Non-photochemical quenching of chlorophyll fluorescence and xanthophyll cycle responses after excess PAR and UVR in *Chaetoceros brevis, Phaeocystis antarctica* and coastal Antarctic phytoplankton. Mar. Ecol. Prog. Ser. 426, 119–131.
Whittaker, K.A., Rignanese, D.R., Olson, R.J., Rynearson, T.A., 2012. Molecular subdivision of the marine diatom *Thalassiosira rotula* in relation to geographic distribution, genome size, and physiology. BMC Evol. Biol. 12, 209.
Yang, E.J., Lee, Y., Lee, S., 2019. Trophic interactions of micro-and mesozooplankton in the Amundsen Sea polynya and adjacent sea ice zone during austral late summer. Prog. Oceanogr. 174, 117–130.
Zapata, M., Rodríguez, F., Garrido, J.L., 2000. Separation of chlorophylls and carotenoids from marine phytoplankton: a new HPLC method using a reversed phase C8 column and pyridine-containing mobile phases. Mar. Ecol. Prog. Ser. 195, 29–45.
Zhu, Z., Xu, K., Fu, F., Spackeen, J.L., Bronk, D.A., Hutchins, D.A., 2016. A comparative study of iron and temperature interactive effects on diatoms and *Phaeocystis antarctica* from the Ross Sea, Antarctica. Mar. Ecol. Prog. Ser. 550, 39–51.